21st Australasian Fluid Mechanics Conference
Adelaide, Australia
10-13 December 2018

Filling Box Flow with Weak Plane Fountain: The Effect of the Reynolds and Prandtl Numbers

Liqiang Dong[1], Wenxian Lin[1,2], S. W. Armfield[3], M. P. Kirkpatrick[3], N. Williamson[3] and Dan Zhao[4]

[1]College of Science & Engineering
James Cook University, Townsville, Queensland 4811, Australia

[2]Solar Energy Research Institute
Yunnan Normal University, Kunming, Yunnan 650092, China

[3]School of Aerospace, Mechanical & Mechatronic Engineering
The University of Sydney, Sydney, New South Wales 2006, Australia

[4]College of Mechanical & Electrical Engineering
Harbin Engineering University, Harbin, Heilongjiang 150001, China

Abstract

This paper studies a filling box flow which results from a weak plane fountain ejected into a semi-confined box with an open top boundary. The fountain is produced by the ejection of dense fluid upwards into a lighter homogeneous ambient fluid at a slot source with uniform velocity. Two-dimensional numerical simulations are carried out to simulate the transient behavior of plane fountains over $5 \leq Re \leq 800$, $0.7 \leq Pr \leq 100$ at $Fr = 1.0$, where Re, Pr and Fr are the Reynolds number, the Prandtl number and the Froude number, respectively. The box has a fixed half bottom length $l = 20$, where l is non-dimensionalized by the source half-width X_0. A gravity current intrusion flow is formed by the reversed flow of the fountain impinging on the bottom, and moves towards the bounded sidewall, resulting in a secondary wall fountain and flow reversal from the sidewall towards the fountain source. Subsequently a time-dependent stratification is produced through convection, filling and thermal conduction. It is found that the effect of Pr considered on the passage of the intrusion is negligible. However, the thickness of the stratified layer varies notably with Pr. Re has significant effects on both the intrusion and the stratification. Scaling correlations are determined for τ_w and V_s, which are the non-dimensional time-scale for the wall fountains to impinge on the side-wall, and the stratification development rate.

Introduction

Fountains, also called negatively buoyant jets, exist widely in both natural and industrial settings. When a jet of dense fluid is ejected upward into a lighter ambient fluid, a fountain is created. The dense flow gradually decelerates under the influence of the opposing buoyant force, and then flows back after it reaches a finite height. The same flow is found in the process where a light jet is discharged downward into a denser ambient fluid. This paper is focused on the upward fountain case.

An intrusion flow results from impingement of the back flow of the fountain on the floor. When the receiving body of the ambient fluid is infinite (that is, not confined), the intrusion flow will behave as a freely spreading gravity current. But in practice a fountain will often occur in a confined space, such as the localized cooling system in buildings and the dense hazardous gases dispersion in limited spaces. In such confined situations the transient behavior of fountain flow is inherently different from that of a freely propagating fountain flow.

In a typical confined fountain case, the intrusion flow impinges on and is turned up by the sidewall, resulting in a secondary wall fountain flow. A reversed flow subsequently moves from the sidewall towards the fountain source due to the stagnation pressure. A stratified structure is then created in the confined space, over a relatively longer time. This process can be described as a 'fountain filling box'. Conversely, the change of the ambient fluid will also affect the behavior of the fountain flow.

It is desirable to be able to predict the transient behavior of the flow produced by generating a fountain flow in a confined region. For example, the capacity to predict the maximum scope of the region where the gas concentrates in the hazardous gas dispersion case will benefit in designing a rescue plan. Hence the factors influencing confined fountains need to be examined. These include the container size, the fountain source geometry and the characteristics of the fountain source, i.e., the momentum flux, and the buoyancy flux.

The influence of the momentum flux and buoyancy flux at the fountain source can be described by Re and Fr, defined for a plane fountain in a homogeneous fluid as,

$$Re = \frac{W_0 X_0}{\nu}, \tag{1}$$

$$Fr = \frac{W_0}{\sqrt{g W_0 (\rho_0 - \rho_a)/\rho_a}} = \frac{W_0}{\sqrt{g \beta W_0 (T_a - T_0)}}, \tag{2}$$

where X_0 is the half-width of the fountain source, W_0 is the mean inlet velocity of the dense jet fluid at the source, g is the acceleration due to gravity, ρ_0, T_0 and ρ_a, T_a are the densities and temperatures of the jet fluid and the ambient fluid at the source, and ν and β are the kinematic viscosity and the coefficient of volumetric expansion of fluid, respectively. In this study the density difference between the jet fluid and ambient fluid results from their temperature difference, and Fr is calculated by the second expression in (2) using the Oberbeck-Boussinesq approximation, which requires the relative density ratio $(\rho_0 - \rho_a)/\rho_0$ to be significantly less than unity. The influence of thermal conduction is quatified by the Prandtl number, which is defined as,

$$Pr = \frac{\nu}{\kappa}, \tag{3}$$

where κ is the thermal diffusivity.

The majority of the existing research has mainly focused on freely propagating fountains, while the confined fountains have received relatively less attention. The problem of releasing buoyant fluid in a confined region was firstly addressed by Baines & Turner [1], which is named as a 'filling box' model by Turner [2]. In the study of Baines & Turner [1], the momentum and buoyancy of the jet flow act in the same direction. As a complement to the 'jet filling box' model, Baines et al., [3] proposed a 'fountain filling box' model by releasing a negatively

buoyant jet in a confined space, which also received more recent attention in recent years (see *e.g.*, [4]). The studies cited above primarily focused on the influence of stratified ambient fluid or density interface on the fountain penetration height, entrainment, and the intrusion speed. However, the evolution of the intrusion flow, wall fountain, reversed flow and stratification is not well studied and thus understood. Particularly, no study has been found to investigate the long-term behavior of confined weak plane fountains, which is the motivation of the current study.

In this study, numerical simulation is used to simulate the behavior of weak plane fountains in an open box over $5 \leq Re \leq 800$ and $0.7 \leq Pr \leq 100$ at $Fr = 1$. The typical evolution of confined fountains is presented. The time series of the intrusion front, wall fountain front and stratification surface are analyzed, and the characteristic time-scale τ_w for the intrusion reaching the sidewall is determined, along with other characterizations of the flow behavior in terms of Re and Pr.

Numerical Method

The computational domain is a rectangular box of width $2L$ and height H as shown in figure. 1, with an open top and no-slip insulated sidewalls. The dense jet is ejected upward from the slot of width $2X_0$ at the bottom center. The remaining bottom is no-slip and insulated. At $t = 0$, the domain is filled with a Newtonian fluid at rest and with a uniform temperature T_a and the dense jet flow is at $T_0 (T_0 < T_a)$ with a uniform velocity W_0. The discharge is maintained thereafter. To remove the influence of the open top boundary, the domain for all the simulations has a ratio of $H/X_0 \geq 20$ and a constant ratio of $L/X_0 = 20$.

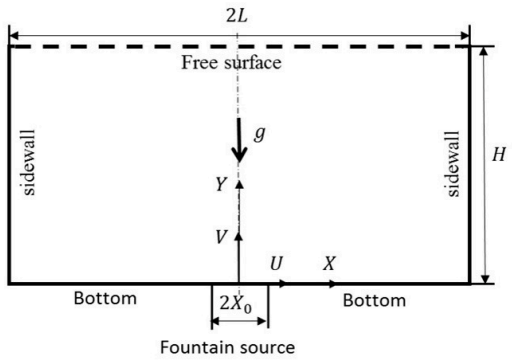

Figure 1: The sketch of the computational domain.

The flow field is obtained by solving the 2D incompressible Navier-Stokes and temperature equations. The equations are discretized on a non-uniform mesh, with the standard 2nd-order central difference schemes used for the viscous and divergence terms and the 3rd-order QUICK scheme for the advective terms. The 2nd-order Adams-Bashforth and Crank-Nicolson schemes are used for the time integration of the advective terms and the diffusive terms, respectively. The PRESTO scheme is used for the pressure gradient. All simulations are performed using ANSYS Fluent 16.

The non-uniform meshes are created using ICEM, with a fine uniform mesh in the region close to the bottom and a relatively coarse stretched mesh in the region near the top. Extensive grid and time-step size dependency tests were undertaken to ensure the accuracy of the results. The result show that the grids of 1336×531 and 4000×1359 cells provide sufficiently accurate solution for the cases with $Re \leq 200$ and $Re \leq 800$ respectively. The non-dimensional time step size $\Delta\tau$ for the simulations is smaller than 0.005, resulting in CFL numbers no more than 0.191.

Results and Discussion

Typical Evolution of Confined Weak Plane Fountain Flows

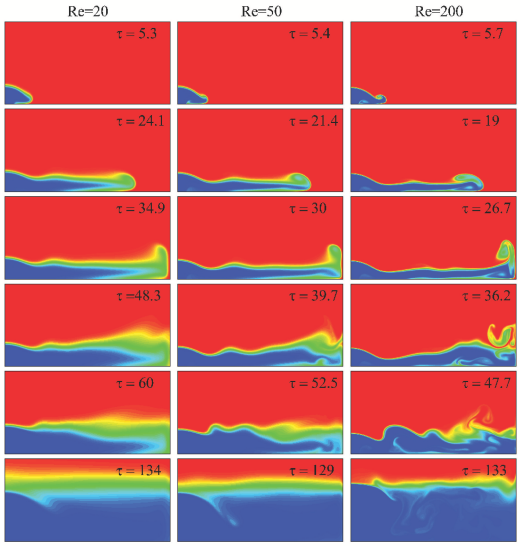

Figure 2: Temperature contours for the fountains of $Fr = 1$ and $Pr = 7$. The left, middle and right columns are for $Re = 20$, $Re = 50$ and $Re = 200$ at six specific times, respectively.

The numerically simulated transient temperature contours are presented in figure 2 for $Fr = 1$ fountains with $Re = 20$, 50 and 200 at six specific times, providing an overview of the evolution of the long-term behavior of weak plain fountains in confined spaces in a homogeneous fluid. Due to the opposing buoyant flux, the dense jet rises to a finite height and then falls back to the floor. Since the backflow of the fountain remains denser than the ambient fluid, a thin current spreading outward results from the impingement of the backflow upon the floor. The depth of the current then has a sudden increase, which can be treated as a hydraulic jump. After that, the intrusion turns into a gravity current. During the spreading process the gravity current's head is thicker than the tailing flow. The gravity current intrusion front subsequently reaches the sidewall and turns upward, forming a wall fountain. Three different models can be used to describe the behavior of the secondary wall fountains. For the $Re = 50$ case, the wall fountain front penetrates a certain height and then slumps down at $\tau = 39.7$. For $Re = 200$ case, the wall fountain front rolls down after reaching the maximum penetration height. There is no falling process observed for the wall fountain with $Re = 20$. As shown at $\tau = 48.3$ in the left column, the wall fountain front is pushed away from the sidewall by the stagnation pressure. For all cases a reversed flow is then created and moves from the sidewall towards the fountain source, interacting with the intrusion flow, ambient fluid and the fountain. Over the long-term, a stratification is created in the box due to convection, filling and thermal conduction, and the fountain is submerged.

Effects of Re on the flow behavior

From figure 2, it is observed that the intrusion is thinner when Re increases during the intrusion stage. This phenomenon is also observed for the $Fr = 1$ fountains at other Re values considered (e.g., $Re = 5, 10, 100, 500$ and 800). The thickness of the thermal layer (the yellow and light blue filled contour in figure

2) of the stratification is also found to decrease with the increase of Re.

Figure 3 shows time series of the location of the intrusion front, determined as the x-location at which the temperature is $T(x) = T_a - 0.01(T_a - T_0)$ within the whole calculation domain. When $Re \leq 200$, the speed of the intrusion is enhanced by increasing Re, but the effects of Re on the intrusion speed is negligible when $Re \geq 500$.

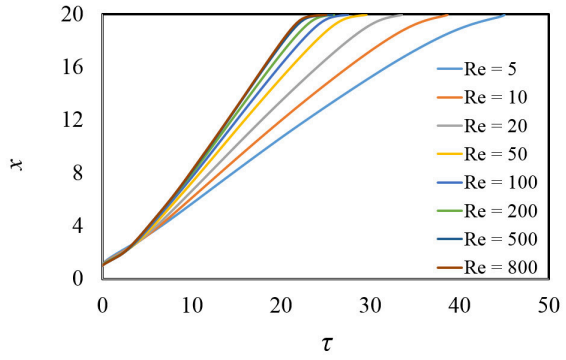

Figure 3: Passage of the intrusion front for a series of Re with $Fr = 1$ and $Pr = 7$, where $x = X/X_0$ and $\tau = (tW_0)/X_0$ are the dimensionless x-location and time.

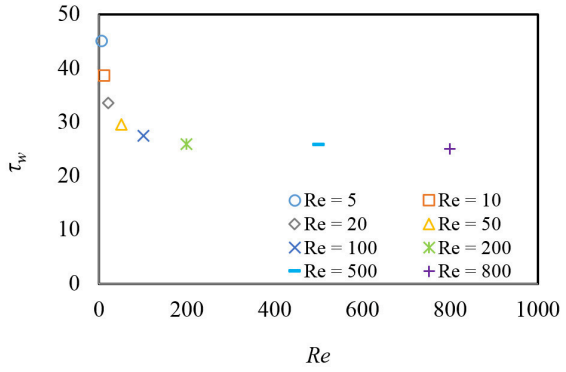

Figure 4: τ_w plotted against Re with $Fr = 1$ and $Pr = 7$.

A characteristic time-scale, τ_w, which is the time instant when the intrusion front impinges on the side-wall, is determined by the end point of the time series as shown in figure 3. The effect of Re on τ_w is shown in figure 4, three ranges are distinguished with three corresponding correlations are determined by power law regression as follows:

$$\tau_w = 63.75Re^{-0.21} - 0.51, \quad \text{for} \quad 5 \leq Re \leq 20, \tag{4}$$

$$\tau_w = 47.52Re^{-0.11} - 0.93, \quad \text{for} \quad 20 \leq Re \leq 200, \tag{5}$$

$$\tau_w = 25.76, \quad \text{for} \quad 200 \leq Re \leq 800, \tag{6}$$

with the regression constants of 0.9995, 0.9935, and 0.9818, respectively.

The thermally stratified surface can be defined as the vertical location where the temperature is $T(x) = T_a - 0.01(T_a - T_0)$. Figure 5 shows time series of the maximum, minimum and averaged heights of the thermally stratified surface after the intrusion reaching the sidewall for $Fr = 1$ and $Re = 200$. The differences among these heights are initially significant, due to the key role played by convection and mixing. The differences decrease and the time series of these heights follow essentially the

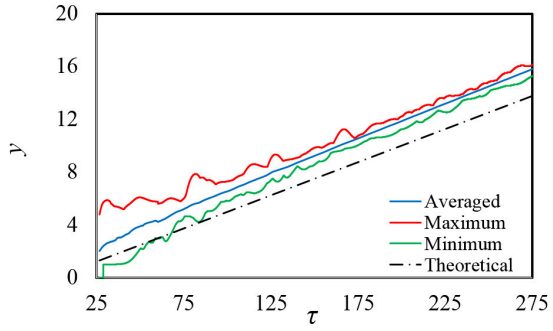

Figure 5: Passage of the thermally stratified surface for the fountain with $Fr = 1.0$, $Re = 200$ and $Pr = 7$.

same trend when filling becomes dominant in the subsequent stratification formation. For a pure filling box, the development rate of the surface, V_s, is the reciprocal of $l = L/X_0$ based on the conservation of mass. From figure 5 it is seen that the development rate of the stratification can be approximately described by the rate of the averaged stratification height profile. Figure 6 presents the development rate of the stratification for fountains over $5 \leq Re \leq 200$, showing notable differences from the theoretical value of $V_s = 1/l = 0.05$. This is because not only filling but also convection and thermal conduction contribute to the development of the stratification. The figure also indicates that the stratification development rate increases with the decease of Re, when thermal conduction has a more significant influence. Power law regression gives the following correlations for V_s,

$$V_s = 0.09Re^{-0.14}, \quad \text{for} \quad 5 \leq Re \leq 20, \tag{7}$$

$$V_s = -0.04Re^{-0.08} + 0.11, \quad \text{for} \quad 20 \leq Re \leq 200, \tag{8}$$

with the regression constants of 0.992 and 0.999 respectively.

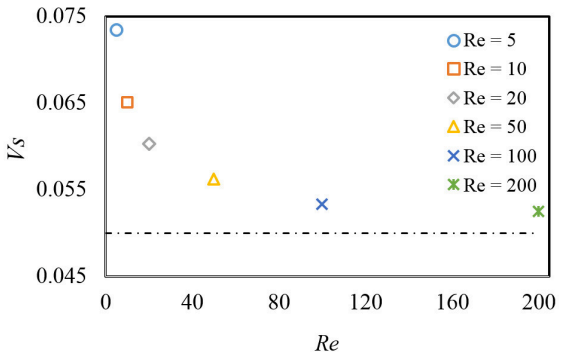

Figure 6: V_s plotted against Re with $Fr = 1$ and $Pr = 7$.

Effects of Pr on the flow behavior

To illustrate the influence of Pr, the temperature contours for fountains with $Fr = 1$, $Re = 200$ and $Pr = 0.7, 7, 10, 20, 50$, and 100 at three stages, are presented in Fig. 7. The left column of figure 7 is the snapshot of temperature contours for the intrusion flows at $\tau = 19$, where a thinner intrusion flow is present when Pr is larger, but the location of the intrusion front is at the same position. This is consistent with the free fountain case as studied by Lin and Armfield (2003) who showed that Pr only influences the thermal layer thickness but has minor effects on the thermal structure [5]. This is also valid for the wall fountain and thermally stratified structure formed at $\tau = 29$ and 133, as shown in the middle and right column of Fig. 7.

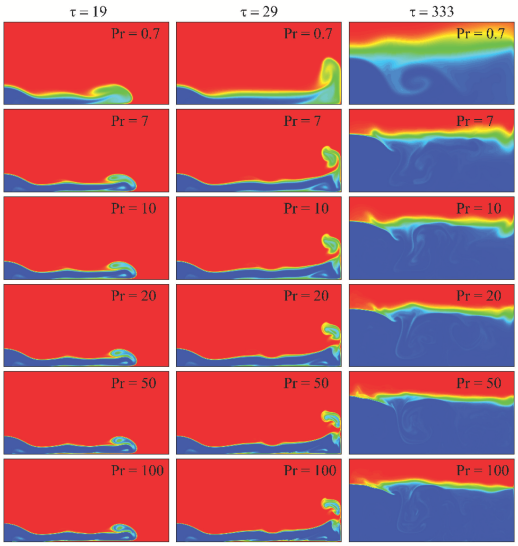

Figure 7: Temperature contours for the fountains of $Fr = 1$ and $Re = 200$ over $0.7 \leq Pr \leq 100$. The left, middle and right columns are for $\tau = 19$, $\tau = 29$ and $\tau = 333$, respectively.

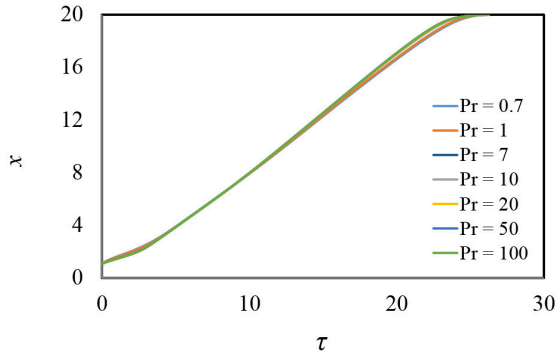

Figure 8: Passage of the intrusion front for a series of Pr with $Fr = 1$ and $Re = 200$.

The time series of the intrusion front over $0.7 \leq Pr \leq 100$ presented in Fig. 8 confirms that the qualitative conclusion that Pr has minor influence on the intrusion front development rate. The development rate of the thermal stratification surfaces are presented in Fig. 9, which can be quantified by the following power law regression relations, showing a weaker influence from thermal conduction with a lager Pr,

$$V_s = 0.06Pr^{0.05} + 0.11, \quad \text{for} \quad 0.7 \leq Pr \leq 10, \tag{9}$$

$$V_s = -0.07Pr^{0.01} + 0.12, \quad \text{for} \quad 10 \leq Pr \leq 100, \tag{10}$$

with the regression constants of 0.9965 and 0.992 respectively.

Conclusions

A 'weak plane fountain filling box' model is developed by the discharge of a weak plane fountain into a confined region in a homogeneous ambient fluid. A series of 2D simulations are carried out to simulate the transient behavior of fountains over the ranges $5 \leq Re \leq 800$ and $0.7 \leq Pr \leq 100$ at $Fr = 1$. A detailed description is given for the typical evolution of the confined weak plane fountains, and three different models (i.e., without falling, slumping down and rolling down) are determined for the wall fountain in terms of Re. The time series of the passage of the intrusion front indicate that the intrusion flow speed increases with increasing Re when $Re \leq 200$,

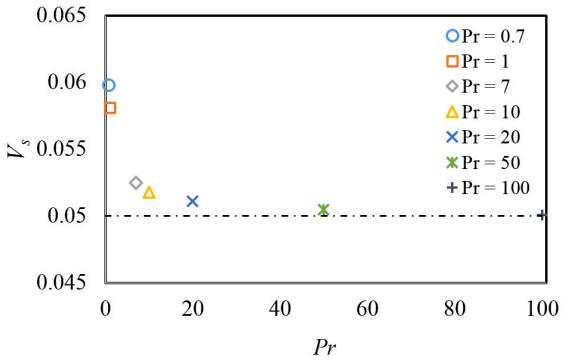

Figure 9: V_s plotted against Pr with $Fr = 1$ and $Re = 200$.

whereas the influence of Pr on the intrusion speed is negligible. The correlations for the characteristic time-scale of the intrusion reaching the sidewall are determined as $\tau_w \sim Re^{-0.21}$ and $\tau_w \sim Re^{-0.11}$ for $5 \leq Re \leq 20$ and $20 \leq Re \leq 200$, respectively, whereas for $200 < Re$ the influence of Re on τ_w is negligible. Convection, filling and conduction all contribute to the formation of thermal stratification. With a smaller Re or Pr, the influence of the thermal conduction becomes more significant. The correlations for the stratification development rate V_s are quantified as $V_s \sim Re^{-0.14}$ and $V_s \sim Re^{-0.08}$ for $5 \leq Re \leq 20$ and $20 \leq Re \leq 200$, respectively. Similarly, $V_s \sim Pr^{0.05}$ and $V_s \sim Pr^{0.01}$ are obtained to quantify the influence of Pr over $0.7 \leq Pr \leq 10$ and $10 \leq Pr \leq 100$, respectively.

Acknowledgements

The support from the Australian Research Council (DP160102134) and the National Natural Science Foundation of China (51469035) is acknowledged. Liqiang Dong acknowledges the financial support of a JCUPRS Scholarship and an Australian Government Research Training Program Scholarship from James Cook University. Dan Zhao also acknowledges the support from the National Natural Science Foundation of China (51775123).

References

[1] Baines, W.D. and Turner, J.S., Turbulent buoyant convection from a source in a confined region, *Journal of Fluid mechanics*, **37(1)**, 1969, 51–80.

[2] Turner, J.S., *Buoyancy effects in fluids*, Cambridge University Press, 1979.

[3] Baines, W.D. Turner, J.S. and and Campbell, I.H., Turbulent fountains in an open chamber, *Journal of Fluid mechanics*, **212**, 1990, 557–592.

[4] Ansong, J.K., Kyba, P.J. and Sutherland, B.R., Fountains impinging on a density interface, *Journal of Fluid mechanics*, **595**, 2008, 115–139.

[5] Lin, W, and Armfield, S.W., The Reynolds and Prandtl number dependence of weak fountains, *Computational Mechanics*, **31(5)**, 2003, 379–389.